ACS APPLIED NANO MATERIALS

www.acsanm.org Article

Electrospun Gold Nanoprism/Poly(vinyl alcohol) Nanofibers for Flexible and Free-Standing Surface-Enhanced Raman Scattering Substrates

Alei Dang,[†] Yuchen Wang,[†] Huiqin Zhang, Weerapha Panatdasirisuk, Yu Xia, Zongyu Wang, Deep Jariwala, Tiehu Li, and Shu Yang*

Cite This: *ACS Appl. Nano Mater.* 2022, 5, 6650−6658 Read Online

ACCESS | Metrics & More | Article Recommendations | Supporting Information

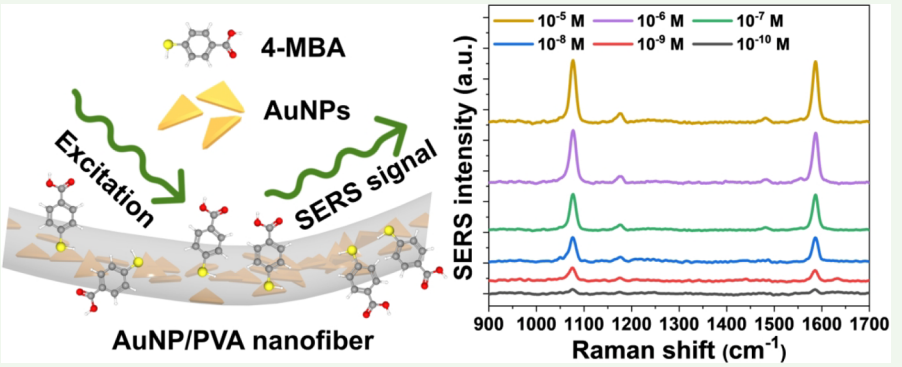

ABSTRACT: Plasmonic resonance from 2D anisotropic metallic nanoparticles for surface-enhanced Raman scattering (SERS) has attracted substantial attention for applications in chemical and environmental monitoring because of its intrinsic electromagnetic "hotspot" and orientation-dependent optical properties. Nevertheless, their sensing applications have been limited by their poor stability toward oxidation and moisture and complicated fabrication processes for large-scale assembly, especially on flexible substrates. In this work, we demonstrate water-stable nanofibers as active SERS substrates electrospun from anisotropic gold nanoprisms (AuNPs) mixed with poly(vinyl alcohol) (PVA) at a concentration of 2.5−20 nM, followed by cross-linking by glutaraldehyde (GA) vapor at room temperature. Using 4-mercaptobenzoic acid (4-MBA) as the target molecule, we show that the nanofiber mat with 20 nM AuNPs exhibits high sensitivity at a concentration as low as 10^{-10} M 4-MBA with an enhancement factor of 10^7 and good uniformity over a very large area (20 cm^2) with an average relative standard deviation of <0.074. The cross-linked PVA/AuNP nanofibers are stable against water without an obvious decrease in the SERS signal. In the detection of Rhodamine 6G (R6G) molecules in the water solution, the Raman intensity of R6G shows almost no decay over 3 months compared to that of the as-prepared mat. Further, we show the detection of trace pesticide (10^{-6} M) on the orange exocarp, suggesting that our fiber mat could be applied for potential applications including food safety, biomedicine, and environmental monitoring.

KEYWORDS: *gold nanoprisms, surface-enhanced Raman scattering, sensing, electrospinning, flexible mat*

INTRODUCTION

With the flourishing advancement of spectroscopy-based analytical techniques, the demand for trace molecular detection has dramatically augmented in a variety of applications, ranging from environmental analysis, food safety, and biomedicine.[1−3] Among the different spectroscopic techniques, surface-enhanced Raman spectroscopy (SERS) has attracted considerable attention because of its simple, rapid, noninvasive, label-free detection of analytes with an extremely low detection limit (up to the single-molecule level).[4,5] To achieve high sensitivity, metallic nanostructures (e.g., from gold and silver) are fabricated as SERS substrates because of the strong electromagnetic enhancement (known as "hotspots") through plasmon coupling between the nearby nanoparticles when the interparticle distance is less than 5 nm.[6] Although nanostructures prepared by top-down approaches offer improved density and uniformity of the "hotspots", they usually suffer from limited spatial resolution and low throughput at a high cost.[7,8] Therefore, bottom-up strategies that can assemble metallic nanostructures into 1D, 2D, and 3D SERS-active substrates are desired.[9]

Received: February 14, 2022
Accepted: April 15, 2022
Published: April 26, 2022

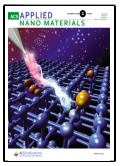

https://doi.org/10.1021/acsanm.2c00689
ACS Appl. Nano Mater. 2022, 5, 6650−6658

Up to now, most nanostructured SERS substrates are fabricated by depositing metallic nanoparticles on rigid SERS substrates, such as glass,[10] alumina,[11] and silicon,[12] thus limiting their potential applications on nonflat surfaces with complex shapes such as wearable devices. Meanwhile, lightweight, portable, and flexible substrates are highly desired.[13,14] Despite the significant efforts in creating flexible SERS substrates from cellulose hydrogels,[15] flexible polymers,[16] tapes,[17] graphene nanosheets,[18] and carbon nanotube sheets,[19] these flexible SERS substrates often suffer from long-term stability and complicated processing procedures with low throughput.[15−18]

Compared to silver (Ag) nanoparticles, gold (Au) nanoparticles show higher resistance to oxidation[20−22] and can adjust the localized surface plasmonic resonance (LSPR) wavelength range from visible to near-infrared (NIR) by controlling their size and morphology.[23] Thus, it is easier to achieve enhanced Raman signals of the probing molecules by matching the maximum plasmonic resonance with the excitation wavelength of the probing laser.[6,23] Several anisotropic Au nanoparticles, such as Au nanorods (AuNRs),[24] Au nanowires (NWs),[25] Au nanocubes,[26] and Au nanoprisms (AuNPs),[12] have been demonstrated as SERS substrates. Among them, AuNPs offer a strong electromagnetic field derived from the dipolar plasmonic resonance at sharp corners and quadrupolar plasmonic resonance at edges and the center with highly reactive facets,[12,23,27−29] However, disadvantages, including long-term stability and complicated processing procedures, limit their widespread applications.

Electrospinning of polymer nanofibers with Au nanoparticles,[30,31] especially anisotropic ones,[32−35] has been considered as one of the most effective methods to generate flexible SERS substrates in a large scale with a high surface-area-to-volume ratio and at a low cost. In general, there are two routes to fabricate anisotropic Au nanoparticle/polymer nanofiber composites via electrospinning. One is to absorb the Au nanoparticles on the outer surface of electrospun nanofibers through electrostatic interactions. For example, Zhu et al.[32] have assembled various Au nanoparticles on functionalized water-stable poly(vinyl alcohol) (PVA)/polyethylenimine nanofibers. However, this method not only requires the nanofibers to be insoluble in the nanoparticle solution but also has a tedious surface modification procedure for both the nanoparticles and nanofibers for successful absorption.[32−34] The SERS enhancement factor (EF), is defined as $EF = \frac{I_{SERS}N_{NR}}{I_{NR}N_{SERS}}$, where I_{SERS} and I_{NR} stand for the intensities of the same vibrational mode in the SERS spectrum and normal Raman spectrum of the analyte and N_{SERS} and N_{NR} are the number of analyte molecules adsorbed on the substrate illuminated by the laser focus spot under SERS and normal Raman conditions. The EF of these SERS substrates is usually reported in the range of $\sim 10^5-10^7$.[32,34] The other approach is to electrospin a nanoparticle/polymer solution. For example, Zhang et al. embedded AuNRs and binary AuNR/AgNW hybrids in a PVA matrix and fabricated freestanding and flexible SERS substrates by electrospinning, where the nanoparticles were stabilized and arranged along the long axis of the PVA nanofibers.[35,36] This approach not only reduces aggregation of the nanoparticles but also decreases the distance between the nearby nanoparticles, thus increasing the number of hotspots for plasmonic coupling. A high EF (e.g., 10^8)[37] is obtained because of the high loading of metallic nanoparticles (e.g., AuNRs, 50−200 nM[35]) or their coassemblies (e.g., a mixture of AuNRs, 10−40 nM, and AgNWs, Ag content 0.0424 M).[36] Nevertheless, the obtained metallic nanoparticle/PVA nanofiber mats can be easily dissolved in an aqueous solution and lose their assembled nanostructures. Overall, it remains challenging to fabricate AuNPs on a flexible substrate over a large area at a low cost, yet with high sensitivity and stability under different environments.

Herein, we demonstrate electrospinning of AuNP/PVA nanofibers as flexible and freestanding SERS substrates over an area larger than 20 cm^2, where the AuNPs are synthesized by the one-pot seedless method using cetyltrimethylammonium chloride as the ligand, showing great compatibility with the PVA matrix. The resulting AuNP/PVA nanofiber mat has high uniformity and reproducibility with a low average relative standard deviation (RSD) value (<0.074) and high sensitivity (10^{-10} M) with an EF of 10^7 toward 4-mercaptobenzoic acid at a loading of 20 nM AuNPs, which is 10 times lower than that reported in the literature (200 nM).[36] A detailed comparison of the EF from the literature versus that in our system can be found in Table S1. Moreover, after cross-linking by glutaraldehyde, the cross-linked PVA/AuNP nanofibers are highly stable against water without an obvious decrease in the SERS signal. The Raman intensity of the Rhodamine 6G/water solution shows almost no decay over 3 months compared to that from the as-prepared mat. Further, we demonstrate the detection of trace pesticide (10^{-6} M) on the orange exocarp.

EXPERIMENTAL SECTION

Materials. Cetyltrimethylammonium chloride (CTAC or $C_{19}H_{42}ClN$; >95%) was purchased from TCI America. Potassium iodide (KI, 99.99%) was purchased from Alfa Aesar. Sodium hydroxide (NaOH; 99.99%) and hydrochloric acid (HCl; 37 wt % in water) were purchased from Fisher Scientific. Poly(vinyl alcohol) (PVA; Mowiol 20-98, M_w = 125000 g mol^{-1}), gold(III) chloride trihydrate ($HAuCl_4 \cdot 3H_2O$), L-ascorbic acid (BioUltra, ≥99.5%), glutaraldehyde (GA; 25% aqueous solution), 4-mercaptobenzoic acid (4-MBA; 99%), thiram (TMTD or tetramethyl thiuram disulfide), and Rhodamine 6G (R6G) were purchased from Sigma-Aldrich. Ultrapure water produced with a Milli-Q Integral 5 system was used in all experiments. All glassware and the stir bar were cleaned with aqua regia [3:1 (v/v) HCl (37%)/HNO_3 (70%) solution], followed by extensive rinsing by deionized (DI) water, and dried before use. All chemicals were used without further purification.

Synthesis and Purification of AuNPs. AuNPs were synthesized by a rapid one-pot seedless growth process with a further purification procedure as reported previously.[12,38,39] Briefly, a 100 mM CTAC aqueous solution was prepared at 40 °C until CTAC was fully dissolved and cooled to room temperature before use. Subsequently, 16 mL of a 100 mM as-prepared CTAC aqueous solution was diluted to 80 mL of water in a 250 mL Erlenmeyer flask, followed by the addition of 0.8 mL of 25.4 mM $HAuCl_4$, 0.75 mL of 10 mM KI, and 0.2 mL of 100 mM NaOH, where a light-yellow solution was formed. The color of the solution changed to colorless after 0.8 mL of 0.064 M ascorbic acid was injected into the solution. Finally, another 0.1 mL of 100 mM NaOH was added to the flask with gentle shaking for 5 s. The solution was left undisturbed at room temperature for 15 min for the growth of AuNPs, and the plasmonic color of the mixture turned from pink to purple and blue.

AuNPs with polyhedral impurities were purified by a depletion-driven method reported in the literature.[12,39] Typically, 10 mL of the reaction products was isolated by centrifugation twice at 5000 rpm for 8 min, followed by decanting of the supernatant. The precipitates were redispersed in 3 mL of DI water for further purification. Subsequently, an aliquot of a 250 mM CTAC aqueous solution was added to the mixture solution (3 mL) until the CTAC concentration reached 150 mM. Finally, the dark-blue solution was left undisturbed for 24 h at room temperature until the supernatant turned purple. Then the supernatant was removed as much as possible from the solution, and the

https://doi.org/10.1021/acsanm.2c00689
ACS Appl. Nano Mater. 2022, 5, 6650−6658

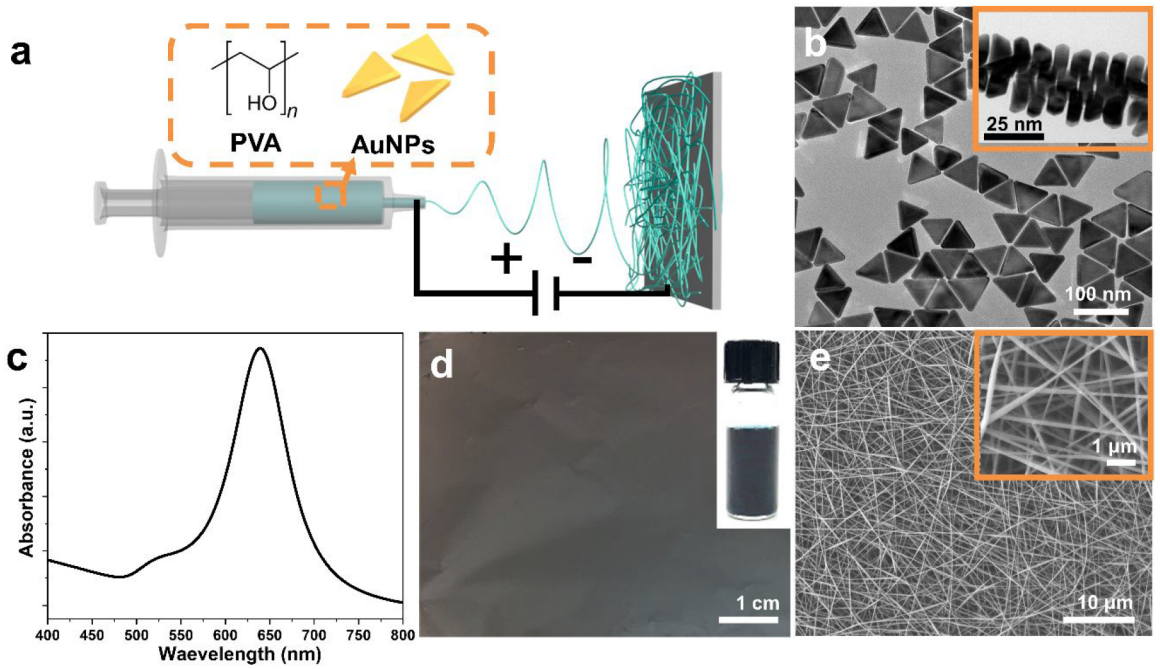

Figure 1. (a) Schematic illustration of the electrospinning process for fabrication of the AuNP/PVA nanofiber mat. (b) TEM image of the AuNPs. Inset: Side-view TEM image of the stacked AuNPs, showing the thickness of the AuNPs. (c) UV−vis spectra of the AuNPs. (d) Photograph of the AuNP/PVA nanofiber mat. Inset: Photograph of a AuNP/PVA (20 nM AuNPs) electrospinning solution. (e) SEM image of the AuNP/PVA mat with an average diameter of ∼178 nm. Inset: SEM image at a higher magnification.

sedimentation was then redispersed in 3 mL of ultrapure water. A large amount of AuNPs for electrospinning was synthesized and purified using the same procedure.

Fabrication of the AuNP/PVA Nanofibers and Cast Films. The desired amount of a dark-green AuNP solution was centrifuged twice at 5000 rpm for 8 min, after which most of the supernatants were removed. The precipitates in the bottom of the centrifuge tube were redispersed in a PVA aqueous solution (7 wt %) under vigorous stirring at room temperature for 4 h until fully dispersed in water. The concentrations of the AuNPs in the PVA solution were 2.5, 5, 10, and 20 nM, respectively. Because of the high hydrophilicity of CTAC coated on the surface of AuNPs, a homogeneous solution of AuNPs and PVA was obtained. Subsequently, the electrospinning solution was fed to a 6 mL plastic syringe with a flat needle tip connected to a high-voltage power supply. A 10 kV voltage and 0.5 mL h^{-1} flow rates at room temperature were used for the electrospinning. The working distance between the needle tip and grounded collector covered by aluminum (Al) foil was 15 cm. To collect the UV−vis absorption spectra of the nanofibers, several pieces of clean glass were stuck onto the collector using conductive tape, and the glass with AuNP/PVA nanofibers was then picked up from the collector for UV−vis measurement. For a comparison of the surface plasmonic resonance of the nanofiber mat and cast films, 50 μL of a AuNP/PVA electrospinning solution with 20 nM AuNPs was drop-cast onto a clean glass substrate and dried under ambient conditions. To collect the SERS spectra at different spinning times, small pieces of Si wafers were taped to the Al foil to collect the AuNP/PVA nanofibers when the collecting time was short and the AuNP/PVA nanofibers were too thin to peel off from the Al foil.

Cross-Linking of the AuNP/PVA Nanofiber Mats. The as-prepared AuNP/PVA nanofiber mats were cross-linked by GA vapor according to the literature.[40] Typically, the AuNP/PVA nanofiber mats were exposed to the 2.5 M GA vapor (pH = 3) in the vacuum desiccator for 48 h, followed by washing with DI water to remove the unreacted GA and drying in a vacuum oven for 24 h.

Fabrication and Measurement of the SERS Samples. The Raman spectra were obtained using a 633-nm-wavelength laser to match the LSPR of AuNPs, and the acquisition time was kept as 5 s for all of the samples. The reflected light signals were collected from the microscope objective (100×) and analyzed using a grating spectrometer coupled to a Si focal plane array. All of these instruments were integrated in the LabRAM HR Evolution Confocal Raman microscope. To prepare the samples for SERS measurement, the resultant AuNP/PVA nanofiber mats peeled off from the Al foil or collected on the Si wafers were immersed in 4-MBA/ethanol solutions with concentrations varying from 10^{-4} to 10^{-10} M. For comparison, 50 μL of a AuNP/PVA electrospinning solution with different AuNP concentrations was also cast onto the Si wafers and immersed in the above 4-MBA/ethanol solutions. The samples were left undisturbed for 4 h and washed with ethanol to remove extra molecules. Then, the AuNP/PVA nanofibers were placed on the Si wafers and dried with all of the other samples. For R6G sensing, the as-spun AuNP/PVA nanofiber mats were immersed in 10^{-4} M R6G/ethanol solutions. The cross-linked AuNP/PVA nanofiber mats were immersed in water for 24 h, followed by immersion in a 10^{-4} M R6G aqueous solution. All of the other procedures were the same as those of the 4-MBA measurement. To estimate the EF, a 10^{-2} M 4-MBA solution was also drop-cast onto the Si wafer and dried at room temperature before the SERS measurement. To measure the trace pesticide, 10^{-6} M TMTD in an acetone solution was sprayed onto small pieces of orange exocarp (1 cm × 1 cm) and dried. Then a drop of pure acetone was dropped onto the orange exocarp, which was then covered by the AuNP/PVA nanofiber mat to collect TMTD. Because the probe molecules could degenerate over time in an external environment, the solutions for SERS were freshly prepared for each test. All of the SERS spectra were collected after baseline correction using a fifth-order polynomial least-squares fitting algorithm to enhance the signal-to-noise ratio.[41]

Characterization. Scanning electron microscopy (SEM; JEOL 7500F HRSEM, operated at 5 kV) and transmission electron microscopy (TEM; JEOL F200, operated at 200 kV) were employed to characterize the structure of the AuNP/PVA nanofibers and size distribution of the AuNPs. To prepare the TEM samples, the copper grids were placed near the grounded collector for ∼10 s, followed by cross-linking if needed. The grids with cross-linked fibers were immersed in water for 24 h, dried, and prepared for characterization. The absorption spectra were recorded by an Agilent Cary 5000 UV−vis−NIR spectrophotometer. The wavelength range was 400−800 nm

https://doi.org/10.1021/acsanm.2c00689
ACS Appl. Nano Mater. 2022, 5, 6650−6658

with an interval of 1 nm, and the scanning rate was 600 nm min^{-1}. The swelling ratio of the solvent-treated nanofibers was calculated by $(d_t - d_{avg})/d_{avg}$, where d_{avg} and d_t are the average diameters of the nanofibers before and after solvent treatment, respectively.

RESULTS AND DISCUSSION

The procedure of fabricating a AuNP/PVA electrospun nanofiber mat is shown in Figure 1a. The AuNPs were synthesized by a rapid one-pot seedless method (see details in the Experimental Section). The UV−vis spectrum of the as-prepared AuNP solution shows a strong absorption peak at 646 nm with a wide shoulder around 500−580 nm in Figure S1c, corresponding to the AuNPs and the polyhedral impurities, respectively. To separate the AuNPs from the polyhedral impurities, a depletion-driven method was employed in the presence of high-concentration CTAC depletants (see details in the Experimental Section).

After purification, the color of the as-prepared solution changes from dark blue to dark green, and the peak intensity from the polyhedral impurities decreases significantly, while the peak of the AuNPs remains. This suggests that the polyhedral impurities are successfully removed, which is further confirmed by TEM images of AuNPs (Figure S1). The resulting AuNPs have an average edge length (l_{avg}) of 59.6 ± 8.7 nm and an average thickness (t_{avg}) of 20.7 ± 1.9 nm, with an LSPR peak at 640 nm (Figures 1b,c and S2). Subsequently, the AuNPs are centrifuged to the desired concentration and mixed with the PVA aqueous solution (7 wt %) for electrospinning.

Electrospinning is known as a facile and cost-effective way to fabricate functional nanofibers on a large scale.[42] Here, a freestanding and flexible AuNP/PVA nanofiber mat over 20 cm^2 is fabricated by electrospinning of a AuNP/PVA solution containing 20 nM AuNPs on Al foil for 30 min (Figure 1d). Because of the random scattering of light from the surface of the nonwoven fibers, the electrospun nanofiber mat appears to be a slightly lighter blue, resulting from the plasmonic color of AuNPs, compared with the dark blue from the AuNP/PVA electrospinning solution. The SEM image confirms the uniformity of the nanofibers with an average diameter (d_{avg}) of around 178 nm and a 3D nonwoven network nature (Figure 1e).

Figure 2 shows the TEM images of AuNP/PVA nanofibers with different concentrations of AuNPs from 2.5 to 20 nM. To better describe the distribution of AuNPs in electrospun nanofibers, the face of AuNPs is defined as the $x-y$ plane, and the perpendicular direction is defined as the z axis (inset of Figure 2a). AuNPs are successfully embedded within the PVA nanofibers and are more likely to be aligned along with the long axis of the nanofibers. The TEM images of the AuNP/PVA nanofibers indicate that the AuNPs have good miscibility with PVA and are uniformly dispersed over the entire nanofiber mat rather than only localized in some nanofibers (Figure S3). As the AuNP concentration increases, the distance between the individual AuNPs decreases, and AuNP dimers start to form when the concentration of AuNPs reaches 5 nM (Figure 2a,b). AuNP trimers and even larger nanoclusters are formed when the concentration of AuNPs reaches 10 and 20 nM (Figure 2c,d). The corresponding SEM images (Figure S4) show that the nanofibers have a smooth surface with relatively uniform diameters. Thus, the randomly dispersed AuNPs in an aqueous solution could be stabilized and "frozen" in PVA nanofibers by the electrospinning process. When a high voltage (10 kV) is applied to the AuNP/PVA solution, a jet under the influence of the flow field erupts from the tip of the spinneret when the repulsive force is larger than the surface tension of the mixture. The jet is bent and stretched because of the synergistic effect of the flow and electric fields, forming nanofibers as water evaporates, which are collected on an Al foil. Here, a flow rate (0.5 mL h^{-1}) is employed to ensure evaporation of water during the electrospinning process.

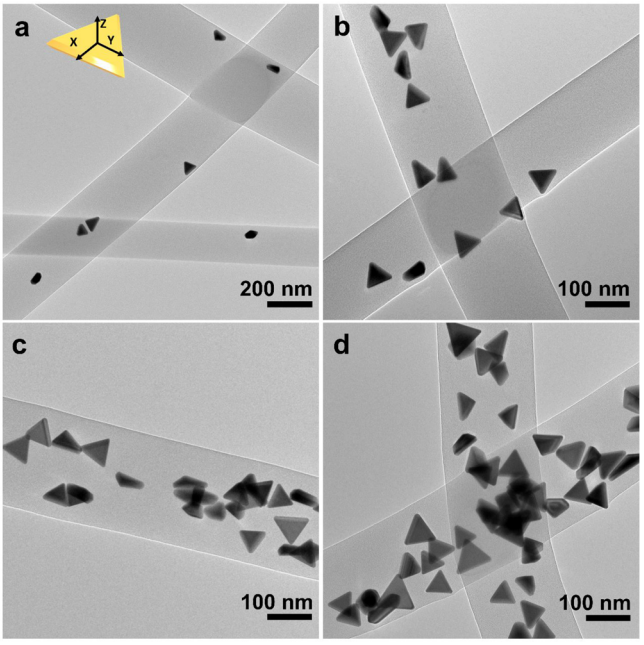

Figure 2. TEM images of the electrospun AuNP/PVA nanofibers with different AuNP concentrations of (a) 2.5, (b) 5, (c) 10, and (d) 20 nM, respectively. Inset in part a: Schematic of the coordinates of AuNPs.

To evaluate the SERS performance of the AuNP/PVA nanofibers, the AuNP/PVA electrospinning solution is drop-cast onto a Si wafer to create a film for comparison (Figure S5). As seen in Figure 3a, the UV−vis absorption peak of the AuNP/PVA nanofiber mat red shifts from 653 to 675 nm compared with the cast film for the same 20 nM AuNP loading amount. This indicates that the interparticle distance of AuNPs in nanofibers decreases under the shearing force due to the electric field during the electrospinning process. Moreover, the peak of the AuNP/PVA nanofiber mat is much broader than that of the cast film, which could be attributed to the plasmonic coupling between the nearby AuNPs in the nanofibers.[43] When the concentration of AuNPs increases from 2.5 to 20 nM, the broad LSPR band shifts from 667 to 675 nm because the plasmonic coupling between AuNPs within the nanofibers further increases because of the formation of larger AuNP clusters at higher loading (Figure 3b). Correspondingly, the relative intensity of the LSPR also increases.

The SERS performance of the AuNP/PVA nanofiber mats and the cast films is characterized by Raman spectrometry using a 632 nm laser to pair with the absorption wavelength of AuNPs. 4-MBA is chosen as the probing molecule to study the plasmonic enhancement of AuNP/PVA nanofibers because it has several distinct Raman features once absorbed onto the AuNP surface. According to the literature, biocompatible PVA polymer nanofibers can slightly swell in an ethanol solution, allowing small 4-MBA molecules to penetrate the PVA nanofibers, migrate to the surface of AuNPs, and eventually access the hotspots between the metallic nanoparticles.[36,44] The same phenomenon is observed in our AuNP/PVA nanofibers, where

https://doi.org/10.1021/acsanm.2c00689
ACS Appl. Nano Mater. 2022, 5, 6650−6658

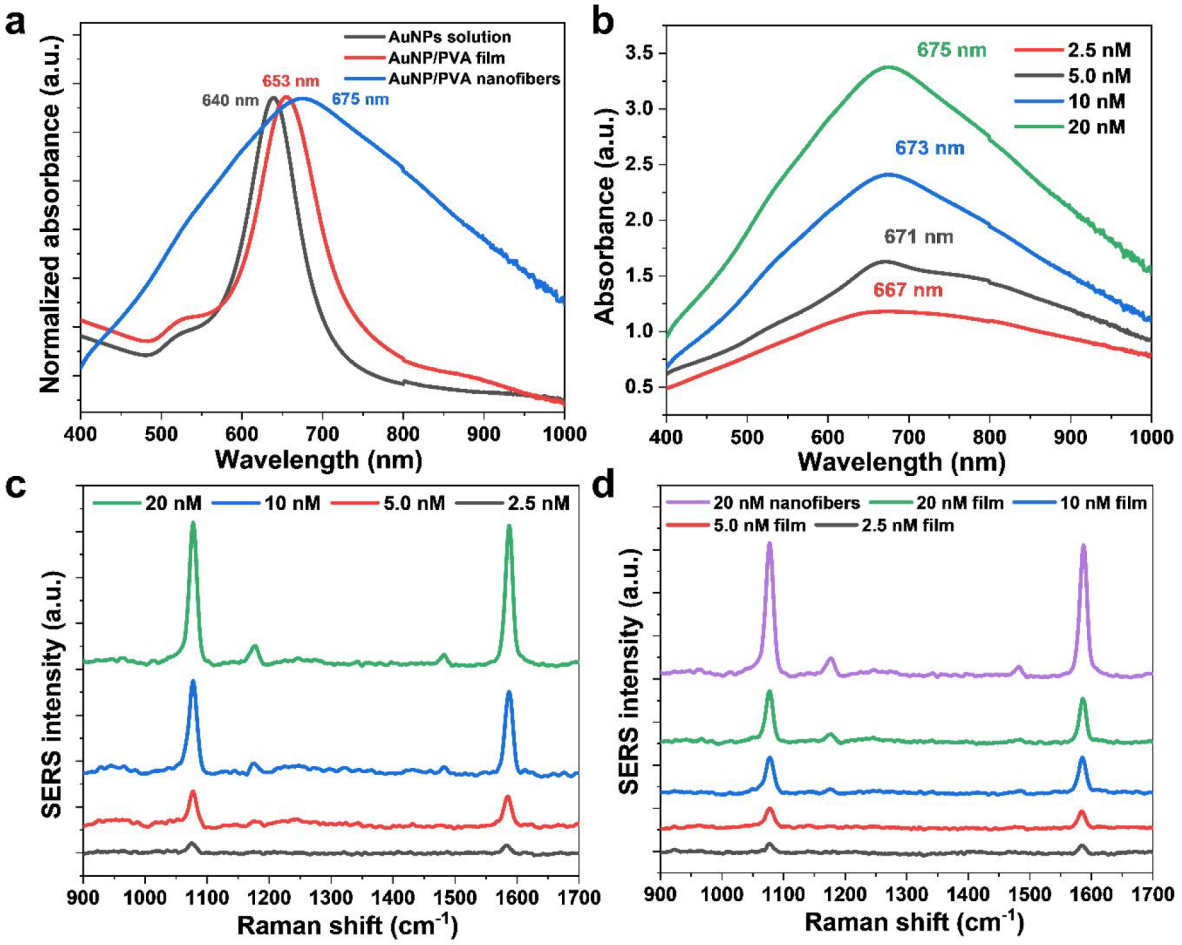

Figure 3. (a) Normalized UV−vis spectra of the electrospun AuNP/PVA nanofiber mat, the AuNP/PVA cast film with 20 nM AuNPs, and the as-synthesized AuNPs in water. (b) UV−vis spectra of AuNP/PVA nanofiber mats with different concentrations of AuNPs. (c) SERS spectra of 10^{-4} M 4-MBA molecules collected on AuNP/PVA nanofiber mats with different concentrations of AuNPs. (d) Comparison of the SERS intensity of the AuNP/PVA nanofiber mat with 20 nM AuNPs and the corresponding AuNP/PVA cast films with different concentrations of AuNPs.

the pristine nanofibers swell 40.6% after ethanol treatment (Figure S6). Figure 3c shows the SERS spectra of 4-MBA molecules (10^{-4} M) absorbed on AuNP/PVA nanofiber mats of different concentrations of AuNPs. A few characteristic Raman bands at 1078, 1178, and 1587 cm^{-1} are observed, attributed to the in-plane ring breathing ν(C−S), the vibration of ν(C−H), and the aromatic ν(C−C), respectively.[45] Clearly, the intensity of the characteristic Raman bands increases as the concentration of the AuNPs increases, suggesting effective plasmonic coupling of the AuNPs at higher concentrations. The SERS spectra of 4-MBA molecules (10^{-4} M) absorbed on the cast AuNP/PVA films show a similar trend (Figure 3d), which can be attributed to the increased total SERS active area in the scattering volume and intercluster coupling effect.[46] The AuNP/PVA nanofiber mat and film show comparable SERS intensities at low AuNP loading (2.5 nM) because the AuNPs are far apart from each other. However, the AuNP/PVA nanofiber mats show much higher SERS intensity than the films as the AuNP concentration increases, which can be explained by the confinement effect of the nanofibers, leading to more AuNP clusters being formed in the nanofiber mat versus in the film at a given AuNP concentration. These Raman spectral results are consistent with the UV−vis spectra.

We then investigate the influence of the electrospinning time. Figure 4a shows a set of SERS spectra of 4-MBA molecules (10^{-4} M) absorbed on the AuNP/PVA nanofiber mats with the same AuNP loading (20 nM) but different electrospinning times. As the thickness of the AuNP/PVA nanofiber mat gradually increases, the intensity of the Raman peak (at 1078 and 1587 cm^{-1}) of 4-MBA molecules increases and plateaus after 30 min (Figure 4b) because the planar intensity of the AuNPs and the number of absorbed probing molecules per unit area of the nanofibers saturate. The optimized AuNP/PVA nanofiber mats prepared by electrospinning the AuNP/PVA solution with 20 nM AuNPs for 30 min are used in the rest of the studies.

The sensitivity and reproducibility of the Raman signals are vital in practical SERS applications. Therefore, we measure the detection limit of 4-MBA on the optimized AuNP/PVA nanofiber mats. As shown in Figure 4c, the characteristic bands of 4-MBA molecules are observed in all of the SERS spectra, where the SERS intensity gradually decreases at lower 4-MBA concentrations. However, the characteristic in-plane ring breathing pattern ν(C−S) at 1078 cm^{-1} and the vibration band of the aromatic ν(C−C) at 1583 cm^{-1} can still be distinctly detected even when the concentration of 4-MBA molecules decreases to 10^{-10} M, indicating the good sensitivity of our nanofiber mat, which can be attributed to a combination of the strong plasmonic coupling between AuNPs with inherently sharp corners and edges and the highly reactive planes of AuNPs. The EF was estimated as 10^7 (see the Supporting Information).

https://doi.org/10.1021/acsanm.2c00689
ACS Appl. Nano Mater. 2022, 5, 6650−6658

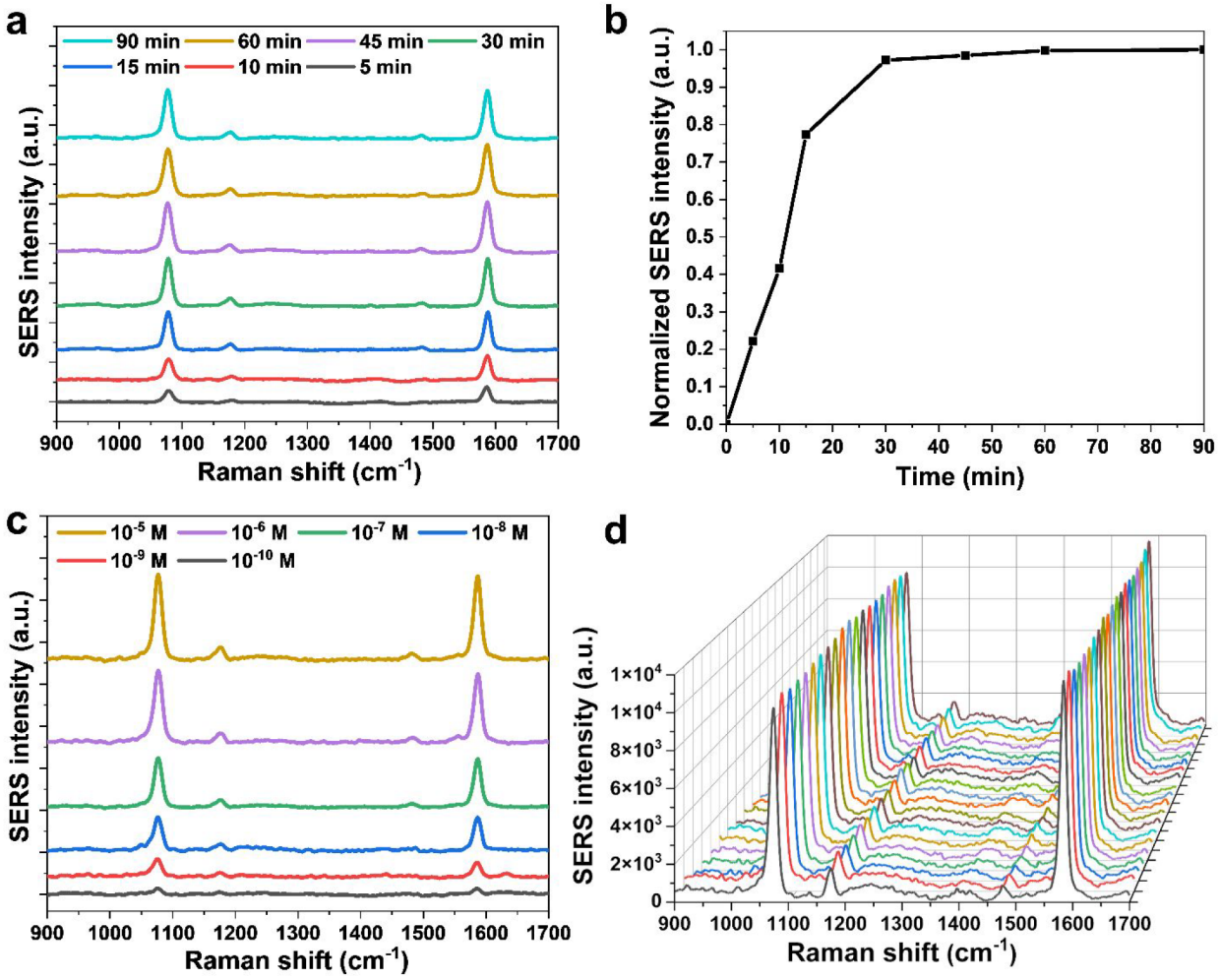

Figure 4. (a) SERS spectra of 10^{-4} M 4-MBA molecules collected on AuNP/PVA nanofiber mats with 20 nM AuNPs at different electrospinning times and (b) the corresponding normalized SERS intensity. (c) SERS spectra of different 4-MBA molecule concentrations absorbed onto the AuNP/PVA nanofiber mats with 20 nM AuNPs. (d) SERS spectra of 10^{-4} M 4-MBA molecules collected at 20 randomly selected spots on the AuNP/PVA nanofiber mat.

To assess the reproducibility and uniformity, SERS spectra of 10^{-4} 4-MBA molecules from 100 randomly selected regions on the AuNP/PVA nanofiber mat were collected (the spectra of 20 random regions are shown in Figure 4d). The average RSD values of 100 Raman peaks are lower than 0.074 (Table 1),

Table 1. RSD Values for the Main Characteristic Raman Bands of 4-MBA on the AuNP/PVA Nanofiber Mat

peak position (cm^{-1})	1078	1178	1587
RSD value	0.053	0.054	0.074

which are less than or comparable to those in previous work,[35,44,47] confirming great reproducibility and uniformity in using AuNP/PVA nanofiber mats as the SERS substrates. Although individual AuNPs or their clusters may not be uniformly dispersed within the single nanofiber (Figure 2), the overall distribution of AuNPs over the entire nanofiber mat is relatively uniform.

We note that the as-prepared AuNP/PVA nanofiber mat can be instantaneously dissolved in water (Video S1), which limits their applications in the detection of analytes used in water or humid environments for bioanalysis and biosensing.[6,15,25] Therefore, we further cross-link the AuNP/PVA nanofiber mats by exposing them to GA vapor at room temperature. The shape of the cross-linked nanofibers is preserved, and the nanofibers swelled by 56.9% after immersion in water for 24 h (Figures 5a and S7). Importantly, AuNPs are still embedded after cross-linking without any morphology changes (Figure 5b). Therefore, the SERS performance will not be affected by the cross-linking step (Figure S8).

To further investigate the universality of the as-prepared substrates and demonstrate the applications in the detection of analytes in water, water-soluble dye R6G is used as a probe molecule. Figure 5c shows strong characteristic peaks of R6G on the water-stable AuNP/PVA nanofiber mat.[48] This indicates that the water-stable AuNP/PVA nanofibers can detect not only 4-MBA in ethanol but also molecules in the aqueous solution. More impressively, the intensity of the main characteristic peaks from R6G shows no obvious shift after 3 months of storage of the nanofibers in air (Figure S9), suggesting that AuNPs are well-protected by cross-linked PVA to resist oxidation compared to nanoparticles immobilized on the outside of electrospun fibers.[32−34] Finally, we demonstrate that our SERS substrate can be applied for the detection of chemicals left on real-world objects. We apply AuNP/PVA nanofiber mats to collect and detect trace pesticide TMTD sprayed on the orange exocarp. As

https://doi.org/10.1021/acsanm.2c00689
ACS Appl. Nano Mater. 2022, 5, 6650−6658

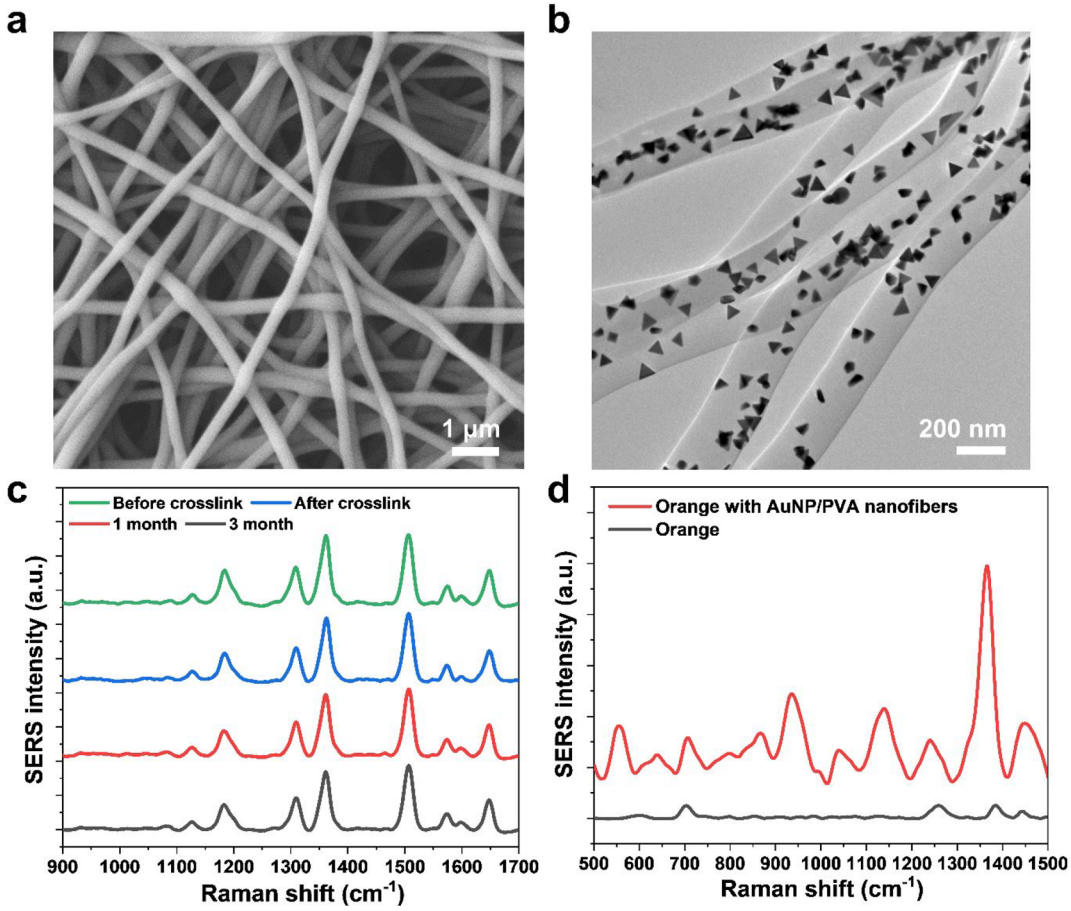

Figure 5. (a) SEM and (b) TEM images of the cross-linked AuNP/PVA nanofibers with 20 nM AuNPs after water treatment for 24 h. (c) SERS spectra of 10^{-4} M R6G molecules collected from the AuNP/PVA nanofiber mat before and after cross-linking and stored in air over 1 and 3 months, respectively. (d) SERS spectra of 10^{-6} M TMTD pesticide sprayed on the orange exocarp, followed by collection using the AuNP/PVA nanofiber mat. Orange with pesticide but without the nanofiber mat wrapping is used as a control sample.

shown in Figure 5d, major peaks at 554, 935, 1140, 1380, and 1524 cm^{-1} can be obtained from the nanofiber mat to detect trace TMTD (1×10^{-6} M) coated on orange exocarp, which is lower than the permissible exposure limit of 5 mg m^{-3} according to the U.S. National Institute for Occupational Safety and Health standard.[49]

CONCLUSION

We present a facile and large-scale approach to fabricating highly sensitive, flexible, freestanding, and water-stable SERS-active substrates with AuNPs by electrospinning AuNPs in a PVA solution. The faces of the AuNPs are arranged along with the long axis of nanofibers as a result of the synergistic effect of the flow field and electric jetting. The Raman signal of 4-MBA probing molecules on AuNP/PVA nanofiber mats with only 20 nM AuNPs is substantially enhanced, achieving an EF of $\sim 10^7$, which is comparable to other literature but with less loading; we attribute it to the electromagnetic enhancement to the "hotspots" (plasmonic coupling) between the nearby AuNPs and from the highly reactive facets of AuNPs. Furthermore, the AuNP/PVA nanofibers display high detection sensitivity (10^{-10} M), reproducibility, and uniformity with the average RSD values of all Raman bands of less than 0.074. After being cross-linked, AuNP/PVA nanofibers are water-stable and show high sensitivity and long-time stability for probing R6G molecules in a water solution without an obvious decrease in the SERS signal. Finally, the detection of trace pesticide (10^{-6} M) on the orange exocarp is demonstrated. This study offers new insights into the incorporation of anisotropic metallic nanoparticles in polymer nanofibers for potential applications in food safety, biomedicine, and environmental monitoring.

ASSOCIATED CONTENT

Supporting Information

The Supporting Information is available free of charge at https://pubs.acs.org/doi/10.1021/acsanm.2c00689.

Estimation of the EF calculation, comparison of different metallic nanoparticle nanofibrous mats for SERS applications, TEM images and UV−vis spectra of the as-prepared AuNPs before and after purification, size and thickness distribution of the AuNPs, TEM and SEM images of electrospinning AuNP/PVA nanofibers with different AuNP concentrations, SEM images of AuNP/PVA nanofibers with 20 nM AuNPs before and after ethanol or water treatment, SERS spectra of 10^{-4} M 4-MBA molecules collected from AuNP/PVA nanofiber mats (20 nM AuNPs) before and after cross-linking, and photographs of AuNP/PVA-cast film and nanofiber mats with 20 nM AuNPs and AuNP/PVA nanofiber mats stored in air over 1 and 3 months (PDF)

https://doi.org/10.1021/acsanm.2c00689
ACS Appl. Nano Mater. 2022, 5, 6650−6658

Video demonstrating the stability of a AuNP/PVA nanofibrous mat (cross-linked and un-cross-linked) in water (AVI)

AUTHOR INFORMATION

Corresponding Author

Shu Yang − *Department of Materials Science and Engineering, University of Pennsylvania, Philadelphia, Pennsylvania 19104, United States;* orcid.org/0000-0001-8834-3320; Email: shuyang@seas.upenn.edu

Authors

Alei Dang − *Department of Materials Science and Engineering, University of Pennsylvania, Philadelphia, Pennsylvania 19104, United States; Shaanxi Engineering Laboratory for Graphene New Carbon Materials and Applications, School of Materials Science and Engineering, Northwestern Polytechnical University, Xi'an 710072, P. R. China*

Yuchen Wang − *Department of Materials Science and Engineering, University of Pennsylvania, Philadelphia, Pennsylvania 19104, United States;* orcid.org/0000-0002-6710-6710

Huiqin Zhang − *Department of Electrical and Systems Engineering, University of Pennsylvania, Philadelphia, Pennsylvania 19104, United States*

Weerapha Panatdasirisuk − *Department of Materials Science and Engineering, University of Pennsylvania, Philadelphia, Pennsylvania 19104, United States*

Yu Xia − *Department of Materials Science and Engineering, University of Pennsylvania, Philadelphia, Pennsylvania 19104, United States*

Zongyu Wang − *Department of Chemistry, Carnegie Mellon University, Pittsburgh, Pennsylvania 15213, United States*

Deep Jariwala − *Department of Electrical and Systems Engineering, University of Pennsylvania, Philadelphia, Pennsylvania 19104, United States;* orcid.org/0000-0002-3570-8768

Tiehu Li − *Shaanxi Engineering Laboratory for Graphene New Carbon Materials and Applications, School of Materials Science and Engineering, Northwestern Polytechnical University, Xi'an 710072, P. R. China*

Complete contact information is available at: https://pubs.acs.org/10.1021/acsanm.2c00689

Author Contributions

†Equal contributions.

Author Contributions

A.D., Y.W., and S.Y. conceived the idea and designed the experiments. A.D. and Y.W. performed the experiments. H.Z., W.P., Y.X., and Z.W. helped with the experiments. T.L., D.J., and S.Y. supervised the work. A.D., Y.W., and S.Y. drafted the manuscript. All of the authors contributed to the editing of the manuscript.

Notes

The authors declare no competing financial interest.

ACKNOWLEDGMENTS

We acknowledge support by the National Science Foundation (NSF) through NSF/INSPIRE Grant IOS-1343159 (to S.Y.), Future Eco Manufacturing Research Grant CMMI 2037097 (to S.Y.), and National Natural Science Foundation of China Grant 52072302 (to A.D.). H.Z. acknowledges partial support from a Vagelos Institute for Energy Science and Technology Graduate Fellowship. The authors also acknowledge the use of SEM, TEM, and Raman as well as a seed grant (to D.J.) supported by the NSF/Materials Research Science and Engineering Center at University of Pennsylvania (Grant DMR-1720530).

REFERENCES

(1) Cecchini, M. P.; Turek, V. A.; Paget, J.; Kornyshev, A. A.; Edel, J. B. Self-assembled nanoparticle arrays for multiphase trace analyte detection. *Nat. Mater.* **2013**, *12* (2), 165−171.

(2) Fahad, H. M.; Shiraki, H.; Amani, M.; Zhang, C.; Hebbar, V. S.; Gao, W.; Ota, H.; Hettick, M.; Kiriya, D.; Chen, Y.-Z.; Chueh, Y.-L.; Javey, A. Room temperature multiplexed gas sensing using chemical-sensitive 3.5-nm-thin silicon transistors. *Sci. Adv.* **2017**, *3* (3), No. e1602557.

(3) Modi, A.; Koratkar, N.; Lass, E.; Wei, B.; Ajayan, P. M. Miniaturized gas ionization sensors using carbon nanotubes. *Nature* **2003**, *424* (6945), 171−174.

(4) Fleischmann, M.; Hendra, P. J.; McQuillan, A. J. Raman spectra of pyridine adsorbed at a silver electrode. *Chem. Phys. Lett.* **1974**, *26* (2), 163−166.

(5) Karthick Kannan, P.; Shankar, P.; Blackman, C.; Chung, C. H. Recent advances in 2D inorganic nanomaterials for SERS sensing. *Adv. Mater.* **2019**, *31* (34), 1803432.

(6) Langer, J.; Jimenez de Aberasturi, D.; Aizpurua, J.; Alvarez-Puebla, R. A.; Auguié, B.; Baumberg, J. J.; Bazan, G. C.; Bell, S. E.; Boisen, A.; Brolo, A. G.; et al. Present and future of surface-enhanced Raman scattering. *ACS Nano* **2020**, *14* (1), 28−117.

(7) Matricardi, C.; Hanske, C.; Garcia-Pomar, J. L.; Langer, J.; Mihi, A.; Liz-Marzan, L. M. Gold Nanoparticle Plasmonic Superlattices as Surface-Enhanced Raman Spectroscopy Substrates. *ACS Nano* **2018**, *12* (8), 8531−8539.

(8) Yang, A.; Hoang, T. B.; Dridi, M.; Deeb, C.; Mikkelsen, M. H.; Schatz, G. C.; Odom, T. W. Real-time tunable lasing from plasmonic nanocavity arrays. *Nat. Commun.* **2015**, *6* (1), 1−7.

(9) Lee, H. K.; Lee, Y. H.; Koh, C. S. L.; Phan-Quang, G. C.; Han, X.; Lay, C. L.; Sim, H. Y. F.; Kao, Y. C.; An, Q.; Ling, X. Y. Designing surface-enhanced Raman scattering (SERS) platforms beyond hotspot engineering: emerging opportunities in analyte manipulations and hybrid materials. *Chem. Soc. Rev.* **2019**, *48* (3), 731−756.

(10) Solís, D. M.; Taboada, J. M.; Obelleiro, F.; Liz-Marzán, L. M.; García de Abajo, F. J. Optimization of nanoparticle-based SERS substrates through large-scale realistic simulations. *ACS Photonics* **2017**, *4* (2), 329−337.

(11) Ko, H.; Chang, S.; Tsukruk, V. V. Porous substrates for label-free molecular level detection of nonresonant organic molecules. *ACS Nano* **2009**, *3* (1), 181−188.

(12) Kim, J.; Song, X.; Ji, F.; Luo, B.; Ice, N. F.; Liu, Q.; Zhang, Q.; Chen, Q. Polymorphic assembly from beveled gold triangular nanoprisms. *Nano Lett.* **2017**, *17* (5), 3270−3275.

(13) Li, Z.; Huang, X.; Lu, G. Recent developments of flexible and transparent SERS substrates. *J. Mater. Chem. C* **2020**, *8* (12), 3956−3969.

(14) Wang, Y.; Zhao, C.; Wang, J.; Luo, X.; Xie, L.; Zhan, S.; Kim, J.; Wang, X.; Liu, X.; Ying, Y. Wearable plasmonic-metasurface sensor for noninvasive and universal molecular fingerprint detection on biointerfaces. *Sci. Adv.* **2021**, *7* (4), No. eabe4553.

(15) Tian, L.; Jiang, Q.; Liu, K. K.; Luan, J.; Naik, R. R.; Singamaneni, S. Bacterial Nanocellulose-Based Flexible Surface Enhanced Raman Scattering Substrate. *Adv. Mater. Interfaces* **2016**, *3* (15), 1600214.

(16) Wu, P.; Zhong, L.-B.; Liu, Q.; Zhou, X.; Zheng, Y.-M. Polymer induced one-step interfacial self-assembly method for the fabrication of flexible, robust and free-standing SERS substrates for rapid on-site detection of pesticide residues. *Nanoscale* **2019**, *11* (27), 12829−12836.

(17) Wang, Y.; Zhang, M.; Feng, L.; Dong, B.; Xu, T.; Li, D.; Jiang, L.; Chi, L. Tape-Imprinted Hierarchical Lotus Seedpod-Like Arrays for

Extraordinary Surface-Enhanced Raman Spectroscopy. *Small* **2019**, *15* (19), 1804527.
(18) Zhao, N.; Cheng, X.; Zhou, Y.; Yang, M.; Yang, J.; Zhong, T.; Zheng, S. Synthesis of flexible free-standing silver nanoparticles-graphene films and their surface-enhanced Raman scattering activity. *J. Nanopart. Res.* **2014**, *16* (4), 1−11.
(19) Xin, W.; Yang, J.-M.; Li, C.; Goorsky, M. S.; Carlson, L.; De Rosa, I. M. Novel strategy for one-pot synthesis of gold nanoplates on carbon nanotube sheet as an effective flexible SERS substrate. *ACS Appl. Mater. Interfaces* **2017**, *9* (7), 6246−6254.
(20) Tang, B.; An, J.; Zheng, X.; Xu, S.; Li, D.; Zhou, J.; Zhao, B.; Xu, W. Silver nanodisks with tunable size by heat aging. *J. Phys. Chem. C* **2008**, *112* (47), 18361−18367.
(21) Tang, B.; Xu, S.; Hou, X.; Li, J.; Sun, L.; Xu, W.; Wang, X. Shape evolution of silver nanoplates through heating and photoinduction. *ACS Appl. Mater. Interfaces* **2013**, *5* (3), 646−53.
(22) Fang, X.; Ren, H.; Zhao, H.; Li, Z. Ultrasensitive visual and colorimetric determination of dopamine based on the prevention of etching of silver nanoprisms by chloride. *Microchimica Acta* **2017**, *184* (2), 415−421.
(23) Reguera, J.; Langer, J.; Jiménez de Aberasturi, D.; Liz-Marzán, L. M. Anisotropic metal nanoparticles for surface enhanced Raman scattering. *Chem. Soc. Rev.* **2017**, *46* (13), 3866−3885.
(24) Zijlstra, P.; Paulo, P. M.; Orrit, M. J. N. n. Optical detection of single non-absorbing molecules using the surface plasmon resonance of a gold nanorod. *Nat. Nanotechnol.* **2012**, *7* (6), 379−382.
(25) Eom, G.; Kim, H.; Hwang, A.; Son, H. Y.; Choi, Y.; Moon, J.; Kim, D.; Lee, M.; Lim, E. K.; Jeong, J.; Huh, Y. M.; Seo, M. K.; Kang, T.; Kim, B. Nanogap-rich Au nanowire SERS sensor for ultrasensitive telomerase activity detection: application to gastric and breast cancer tissues diagnosis. *Adv. Funct. Mater.* **2017**, *27* (37), 1701832.
(26) Omar, R.; En Naciri, A.; Jradi, S.; Battie, Y.; Toufaily, J.; Mortada, H.; Akil, S. One-step synthesis of a monolayer of monodisperse gold nanocubes for SERS substrates. *J. Mater. Chem. C* **2017**, *5* (41), 10813−10821.
(27) Chowdhury, E.; Rahaman, M. S.; Sathitsuksanoh, N.; Grapperhaus, C. A.; O'Toole, M. G. DNA-induced assembly of gold nanoprisms and polystyrene beads into 3D plasmonic SERS substrates. *Nanotechnology* **2021**, *32* (2), 025506.
(28) Lee, Y. H.; Lee, C. K.; Tan, B.; Rui Tan, J. M.; Phang, I. Y.; Ling, X. Y. Using the Langmuir-Schaefer technique to fabricate large-area dense SERS-active Au nanoprism monolayer films. *Nanoscale* **2013**, *5* (14), 6404−6412.
(29) Kuttner, C.; Mayer, M.; Dulle, M.; Moscoso, A.; Lopez-Romero, J. M.; Forster, S.; Fery, A.; Perez-Juste, J.; Contreras-Caceres, R. Seeded Growth Synthesis of Gold Nanotriangles: Size Control, SAXS Analysis, and SERS Performance. *ACS Appl. Mater. Interfaces* **2018**, *10* (13), 11152−11163.
(30) Liu, Z.; Yan, Z.; Jia, L.; Song, P.; Mei, L.; Bai, L.; Liu, Y. Gold nanoparticle decorated electrospun nanofibers: A 3D reproducible and sensitive SERS substrate. *Appl. Surf. Sci.* **2017**, *403*, 29−34.
(31) Sang, Y.; Chen, X.; Zhang, L.; Li, D.; Xu, H. Electrospun polymeric nanofiber decorated with sea urchin-like gold nanoparticles as an efficient and stable SERS platform. *J. Colloid Interface Sci.* **2021**, *590*, 125−133.
(32) Zhu, H.; Du, M.; Zhang, M.; Wang, P.; Bao, S.; Zou, M.; Fu, Y.; Yao, J. Self-assembly of various Au nanocrystals on functionalized water-stable PVA/PEI nanofibers: a highly efficient surface-enhanced Raman scattering substrates with high density of "hot" spots. *Biosens. Bioelectron.* **2014**, *54*, 91−101.
(33) Lee, C. H.; Tian, L.; Abbas, A.; Kattumenu, R.; Singamaneni, S. Directed assembly of gold nanorods using aligned electrospun polymer nanofibers for highly efficient SERS substrates. *Nanotechnology* **2011**, *22* (27), 275311.
(34) Tang, W.; Chase, D. B.; Rabolt, J. F. Immobilization of gold nanorods onto electrospun polycaprolactone fibers via polyelectrolyte decoration-a 3D SERS substrate. *Anal. Chem.* **2013**, *85* (22), 10702−9.
(35) Zhang, C. L.; Lv, K. P.; Cong, H. P.; Yu, S. H. Controlled assemblies of gold nanorods in PVA nanofiber matrix as flexible free-standing SERS substrates by electrospinning. *Small* **2012**, *8* (5), 648−653.
(36) Zhang, C.-L.; Lv, K.-P.; Huang, H.-T.; Cong, H.-P.; Yu, S.-H. Co-assembly of Au nanorods with Ag nanowires within polymer nanofiber matrix for enhanced SERS property by electrospinning. *Nanoscale* **2012**, *4* (17), 5348−5355.
(37) Zhao, X.; Li, C.; Li, Z.; Yu, J.; Pan, J.; Si, H.; Yang, C.; Jiang, S.; Zhang, C.; Man, B. In-situ electrospun aligned and maize-like AgNPs/PVA@Ag nanofibers for surface-enhanced Raman scattering on arbitrary surface. *Nanophotonics* **2019**, *8* (10), 1719−1729.
(38) Chen, L.; Ji, F.; Xu, Y.; He, L.; Mi, Y.; Bao, F.; Sun, B.; Zhang, X.; Zhang, Q. High-yield seedless synthesis of triangular gold nanoplates through oxidative etching. *Nano Lett.* **2014**, *14* (12), 7201−7206.
(39) Scarabelli, L.; Coronado-Puchau, M.; Giner-Casares, J. J.; Langer, J.; Liz-Marzan, L. M. Monodisperse gold nanotriangles: size control, large-scale self-assembly, and performance in surface-enhanced Raman scattering. *ACS Nano* **2014**, *8* (6), 5833−5842.
(40) Destaye, A. G.; Lin, C.-K.; Lee, C.-K. interfaces. Glutaraldehyde vapor cross-linked nanofibrous PVA mat with in situ formed silver nanoparticles. *ACS Appl. Mater. Interfaces* **2013**, *5* (11), 4745−4752.
(41) Yang, T.; Ma, J.; Zhen, S. J.; Huang, C. Z. Electrostatic Assemblies of Well-Dispersed AgNPs on the Surface of Electrospun Nanofibers as Highly Active SERS Substrates for Wide-Range pH Sensing. *ACS Appl. Mater. Interfaces* **2016**, *8* (23), 14802−11.
(42) Zhang, C.-L.; Yu, S.-H. Nanoparticles meet electrospinning: recent advances and future prospects. *Chem. Soc. Rev.* **2014**, *43* (13), 4423−4448.
(43) Lee, D.-R.; Hong, S.-C.; Park, S.-H. Controlled Assembly of Gold Nanoprism and Hexagonal Nanoplate Films for Surface Enhanced Raman Scattering. *Bull. Korean Chem. Soc.* **2011**, *32* (10), 3575−3580.
(44) Zhang, C. L.; Lv, K. P.; Hu, N. Y.; Yu, L.; Ren, X. F.; Liu, S. L.; Yu, S. H. Macroscopic-scale alignment of ultralong Ag nanowires in polymer nanofiber mat and their hierarchical structures by magnetic-field-assisted electrospinning. *Small* **2012**, *8* (19), 2936−2940.
(45) Zhang, X.-Y.; Han, D.; Pang, Z.; Sun, Y.; Wang, Y.; Zhang, Y.; Yang, J.; Chen, L. Charge transfer in an ordered Ag/Cu2S/4-MBA system based on surface-enhanced Raman scattering. *J. Phys. Chem. C* **2018**, *122* (10), 5599−5605.
(46) Yan, B.; Thubagere, A.; Premasiri, W. R.; Ziegler, L. D.; Dal Negro, L.; Reinhard, B. M. Engineered SERS substrates with multiscale signal enhancement: nanoparticle cluster arrays. *ACS Nano* **2009**, *3* (5), 1190−1202.
(47) He, D.; Hu, B.; Yao, Q.-F.; Wang, K.; Yu, S.-H. Large-scale synthesis of flexible free-standing SERS substrates with high sensitivity: electrospun PVA nanofibers embedded with controlled alignment of silver nanoparticles. *ACS Nano* **2009**, *3* (12), 3993−4002.
(48) Watanabe, H.; Hayazawa, N.; Inouye, Y.; Kawata, S. DFT vibrational calculations of rhodamine 6G adsorbed on silver: analysis of tip-enhanced Raman spectroscopy. *J. Phys. Chem. B* **2005**, *109* (11), 5012−5020.
(49) NIOSH Pocket Guide to Chemical Hazards. https://www.cdc.gov/niosh/npg/npgd0612.html (accessed 2022).

https://doi.org/10.1021/acsanm.2c00689
ACS Appl. Nano Mater. 2022, 5, 6650−6658